

Correlation Effects in Quantum Dot Wave Function Imaging

Massimo Rontani¹ and Elisa Molinari^{1,2}¹INFM-CNR National Research Center on nanoStructures and bioSystem s at Surfaces (S3), Modena, Italy²Dipartimento di Fisica, Università degli Studi di Modena e Reggio Emilia, Via Campi 213/A, 41100 Modena, Italy

We demonstrate that in semiconductor quantum dots wave functions, as imaged by local tunneling spectroscopies like STM, show characteristic signatures of electron-electron Coulomb correlation. We predict that such images correspond to "quasi-particle" wave functions which cannot be computed by standard mean-field techniques in the strongly correlated regime. From the configuration-interaction solution of the few-particle problem for prototype dots, we find that quasi-particle wavefunction images may display signatures of Wigner crystallization.

KEYWORDS: STM, tunneling spectroscopies, semiconductor quantum dots, electron solid, configuration interaction

1. Introduction

Present single-electron tunneling spectroscopies in semiconductor quantum dots¹⁽³⁾ (QDs) provide spectacular images of QD wave functions.⁴⁽⁹⁾ The measured intensities are generally identified with the density of carrier states at the resonant tunneling (Fermi) energy, resolved in either real⁴⁽⁶⁾ or reciprocal⁷⁽⁹⁾ space. However, Coulomb blockade phenomena and strong inter-carrier correlation, which are the fingerprints of QD physics, complicate the above simple picture.¹⁰⁾ Indeed, QDs can be strongly interacting objects with a completely discrete energy spectrum, which in turn depends on the number of electrons,^{1,3)} N . Therefore, orbitals can be ill-defined, losing their meaning due to interaction. Also, it is unclear how many electrons one should take into account to calculate the local density of states, as a particle tunnels into a QD and the number of electrons filling the dot fluctuates between $N-1$ and N (such fluctuation is the origin of either the Coulomb current peak or the capacitive signal).^{9,11(13)}

Here we clarify the physical quantities actually probed by scanning tunneling microscopies⁴⁽⁶⁾ (STM) or magnetotunneling spectroscopies^{7(9,11)} of QDs, and how they depend on interactions. If only one many-body state is probed at a time, then the signal is proportional to the probability density of the quasi-particle (QP) being injected into the interacting QD. We demonstrate that the QP density dramatically depends on the strength of correlation inside the dot, and it strongly deviates from the common mean-field (density functional theory, Hartree-Fock) picture in physically relevant regimes.

2. Theory of Quasi-Particle Imaging

The imaging experiments, in their essence, measure quantities directly proportional to the probability for transfer of an electron through a barrier, from an emitter, where electrons fill in a Fermi sea, to a dot, with completely discrete energy spectrum. In multi-terminal setups one can neglect the role of electrodes other than the emitter, to a first approximation. The measured quantity can be the current,^{4,7)} the differential conductance,^{5,6,8,12)} or the QD capacitance,^{9,11,13)} while the emitter can be the STM tip,⁴⁽⁶⁾ or a n-doped GaAs con-

tact,^{7(9,11(13)} and the barrier can be the vacuum⁴⁽⁶⁾ as well as a AlGaAs spacer.^{7(9,11(13)}

According to the seminal paper by Bardeen,¹⁴⁾ the transition probability (at zero temperature) is given by the expression $(2\pi\hbar)^{-1} |M|^2 n(\epsilon)$, where M is the matrix element and $n(\epsilon)$ is the energy density of the final QD states. The common wisdom would predict the probability to be proportional to the total density of QD states at the resonant tunneling energy, ϵ , possibly space-resolved since M would depend on the resonant QD orbital.¹⁵⁾ Let us now assume that: (i) Electrons in the emitter do not interact and their energy levels form a continuum. (ii) Electrons from the emitter access through the barrier a single QD at a sharp resonant energy, corresponding to a well defined interacting QD state. (iii) The x and y motions of electrons are separable, the z axis being parallel to the tunneling direction. (iv) Electrons in the QD all occupy the same confined orbital along z , $\phi_D(z)$. Then one can show¹⁰⁾ that the matrix element M may be factorized as

$$M = T / M; \quad (1)$$

where T is a purely single-particle matrix element while the integral M contains the whole correlation physics.

The former term is proportional to the current density evaluated at any point z_{bar} in the barrier:

$$T = \frac{\hbar^2}{2m} \left[\psi_E(z) \frac{\partial \phi_D(z)}{\partial z} - \phi_D(z) \frac{\partial \psi_E(z)}{\partial z} \right]_{z=z_{\text{bar}}}; \quad (2)$$

where $\psi_E(z)$ is the resonating emitter state along z evanescent in the barrier and m is the electron effective mass. The term (2) contains the information regarding the overlap between emitter and QD orbital tails in the barrier, $\psi_E(z)$ and $\phi_D(z)$, respectively. Since T is substantially independent from both N and xy location, its value is irrelevant in the present context.

On the other hand, the in-plane matrix element M conveys the information related to correlation effects:

$$M = \int \psi_D(\%)' \phi_D(\%) d\%; \quad (3)$$

where $\psi_D(\%)'$ is the QP wavefunction of the interacting QD system:⁴⁽⁶⁾

$$\psi_D(\%) = \hbar N \sum_i j^i(\%) \phi_i; \quad (4)$$

Here ψ_E is the in-plane part of the emitter resonant orbital, $\hat{c}_i(\%)$ is the fermionic field operator destroying an electron at position $\% = (x; y)$, $|N-1\rangle$ and $|N\rangle$ are the QD interacting ground states with $N-1$ and N electrons, respectively (see also Sec. 3). We omit spin indices for the sake of simplicity.

Results (3-4) are the key for predicting wave function images both in real and reciprocal space. In STM, $\psi_E(\%)$ is the localized tip wave function; if we ideally assume it point-like and located at $\%_0$,¹⁵⁾ i.e. $\psi_E(\%) = \delta(\% - \%_0)$, then the signal intensity is proportional to $|\psi_{QD}(\%_0)|^2$, which is the usual result of the one-electron theory,^{6,15)} provided the ill-defined QD orbital is replaced by the QP wavefunction unambiguously defined by Eq. (4). In magnetotunneling spectroscopy, the emitter in-plane wavefunction is a plane wave, $\psi_E(\%) = e^{ik\%}$, and the matrix element (3) is the Fourier transform of ψ_{QD} , $M = \psi_{QD}(k)$. Again, we generalize the standard one-electron result⁸⁾ by substituting $\psi_{QD}(k)$ for the QD orbital. Note that M is the relevant quantity also for intensities in space-integrated spectroscopies probing the QD addition energy spectrum.^{12,13)}

3. Two-dimensional Quantum Dot

3.1 The Non-Interacting Case

We now apply the theory of Sec. 2 to a two-dimensional parabolic QD with a few strongly interacting electrons. The harmonic potential was proven to be an excellent description of several experimental traps.³⁾ The non-interacting effective-mass Hamiltonian of the i -th electron is

$$H_0(i) = \frac{p_i^2}{2m} + \frac{1}{2}m\omega_0^2 r_i^2 \quad (5)$$

The eigenstates $\psi_a(\%)$ of (5) are known as Fock-Darwin orbitals.¹⁷⁾ Their peculiar shell structure, with constant energy spacing $\sim \hbar\omega_0$, is represented in Fig. 1 up to the third shell.

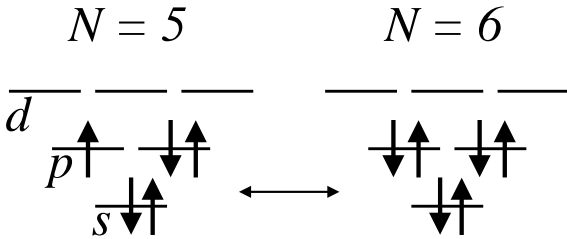


Fig. 1. Electronic configuration of the non-interacting quantum dot ground state as the electron number, N , fluctuates between 5 and 6. The arrows represent electrons (with their spin) filling Fock-Darwin orbitals. The letters identify different energy shells (the third-shell central orbital has s character).

What is $\psi_{QD}(\%)$ in the non-interacting case? Let us consider e.g. $N = 6$. Then, the 5-electron ground state $|N-1\rangle$ appearing in the definition (4) is naturally obtained from the Aufbau principle of atomic physics:¹²⁾ all and only the lowest-energy Fock-Darwin orbitals are

filled with electrons according to Pauli exclusion principle (left panel of Fig. 1). The 6-electron ground state $|N\rangle = \hat{c}_p^\dagger |N-1\rangle$ is obviously obtained from $|N-1\rangle$ by adding a spin-up electron into the lowest-energy p -type empty orbital (right panel of Fig. 1); here \hat{c}_p^\dagger is the pertinent creation operator. By expanding the field operator $\hat{\psi}$ on the Fock-Darwin orbital basis, $\hat{\psi}(\%; s_z) = \sum_a \psi_a(\%) (s_z) \hat{c}_a (s_z)$ is the spin part of the electron wave function with eigenvalue $\epsilon_a = \hbar\omega_0/2$ and spin coordinate s_z , we derive that the orbital part of the QP wave function is simply $\psi_{QD}(\%) = \psi_p(\%)$.

The above result is a sensible one: as we inject e.g. via the STM tip an additional electron to the 5-electron ground state and N oscillates between 5 and 6 (Fig. 1), the non-interacting wave function of the tunneling electron can be regarded alternatively either as the lowest-energy unoccupied orbital when $N = 5$ (Fig. 1 left panel) or as the highest-energy occupied orbital when $N = 6$ (Fig. 1 right panel). In the section below we consider the effects of electron-electron interaction.

3.2 Configuration-Interaction Approach to the Interacting Problem

The fully interacting Hamiltonian is the sum of single-particle terms (5) plus the Coulomb term:

$$H = \sum_{i=1}^N H_0(i) + \frac{1}{2} \sum_{i \neq j} \frac{e^2}{\epsilon_0 \epsilon_r |\%_i - \%_j|}; \quad (6)$$

where ϵ_r is the static relative dielectric constant of the host semiconductor. We solve numerically the few-body problem of Eq. (6), for the ground state at different N 's, by means of the configuration interaction (CI) method,¹⁷⁽¹⁹⁾ where $|N\rangle$ is expanded in a series of Slater determinants built by filling in a truncated set of Fock-Darwin orbitals with N electrons, and consistently with symmetry constraints. From the solution of the resulting large-size matrix-diagonalization problem, we obtain eigenvalues and eigenvectors of ground- and first excited-states.²⁰⁾ Then, we evaluate the matrix element (4), by decomposing $|N-1\rangle$ and $|N\rangle$ on the Slater determinant basis: the resulting $\psi_{QD}(\%)$ is now a mixture of different Fock-Darwin orbitals, with weights controlled by the strength of correlation.

3.3 Tuning the Strength of Correlation

A way of artificially tuning the strength of Coulomb correlation in QDs is to dilute the electron density. While the kinetic energy term scales as r_s^{-2} , r_s being the parameter measuring the average distance between electrons, the Coulomb energy scales as r_s^{-1} . Therefore, at low enough density, electrons pass from a "liquid" phase, where low-energy motion is equally controlled by kinetic and Coulomb energy, to a "crystallized" phase, reminiscent of the Wigner crystal in the bulk, where electrons are localized in space and arrange themselves in a geometrically ordered configuration such that electrostatic repulsion is minimized.³⁾ In the latter regime Coulomb correlation severely mixes many different Slater determinants, and the CI approach is the ideal tool to quantitatively predict correlation effects.¹⁷⁾

The typical QD lateralextension is given by the characteristic dot radius $\ell_D = (\gamma m \ell_0)^{1/2}$, ℓ_D being the mean square root of γ on the Fock-Darwin lowest-energy level γ_s . As we keep N fixed and increase ℓ_D , the Coulomb-to-kinetic energy ratio $\gamma = \ell_D^2/a_B$ [$a_B = \hbar^2/(m e^2)$] is the effective Bohr radius of the dot²¹⁾ increases as well, driving the system into the "Wigner" regime.²²⁾ As a rough indication, consider that for $\gamma \lesssim 2$ or lower the electronic ground state is liquid, while above 4 electrons form a "crystallized" phase.²¹⁾

4. From high to low electron density: Wigner crystallization

Figure 2 shows the square modulus of the QP wave function, corresponding to the injection of the 6-th electron, in the xy plane for three different values of γ . As γ increases (from top to bottom), the density decreases going from the non-interacting limit (Fig. 2, top panel, $\gamma = 0.5$), deep into the Wigner regime (Fig. 2, bottom panel, $\gamma = 10$). At high density ($\gamma = 0.5$, approximately corresponding to the electron density $n_e = 3.8 \times 10^{12} \text{ cm}^{-2}$) the wave function substantially coincides with the non-interacting Fock-Darwin p-orbital $\psi_p(\gamma)$ of Fig. 1. By increasing the QD radius (and γ), the QP wave function weight moves towards larger values of γ . By measuring lengths in units of ℓ_D , as it is done in Fig. 2, this trivial effect should be totally compensated. However, we see in the middle panel of Fig. 2 ($\gamma = 4$, $n_e = 1.5 \times 10^{10} \text{ cm}^{-2}$) that the now much stronger correlation is responsible for an unexpected weight reorganization, which is related to the formation of an outer "ring" of crystallized electrons in the Wigner molecule.²¹⁾ Such tendency is clearly confirmed at even lower densities ($\gamma = 10$, $n_e = 1.3 \times 10^9 \text{ cm}^{-2}$). Now, together with the outer ring, a new structure is visible close to the QD center (if $\gamma \neq 0$ then $\psi_{QP} \neq 0$ due to the orbital p-symmetry). Such complex shape is consistent with the onset of a solid phase with 5 electrons sitting at the apices of a regular pentagon plus one electron at the center.^{21,23,24)}

In Fig. 2 the absolute QP weight has been arbitrarily renormalized, which we believe to be a sensible procedure in view of comparison with experimental images. In order to illustrate a second correlation effect, in addition to shape changes, in Fig. 3 we plot the absolute value of the QP wave function as a function of x at $y = 0$, for the same values of γ as in Fig. 2.¹⁰⁾ Figure 3 clearly demonstrates a dramatic weight loss as γ is increased: the stronger the correlation, the more effective the orthogonality between interacting states. Note also in Fig. 3 that the shoulder of the outer QP peak close to the QD center is clearly visible for $\gamma = 10$.

5. Present Status of Imaging Experiments

Among the existing imaging tunneling experiments,^{4(6,8,9,11)} two have specially focused on results in the presence of several carriers in the QD.^{9,11)}

A first experiment⁹⁾ concerned electrons in InAs self-assembled QDs in the non-interacting high-density limit ($\gamma = 0.5$). This work demonstrates the experimental imaging of an Aufbau-like filling sequence as up to six electrons are sequentially injected into the QDs. In par-

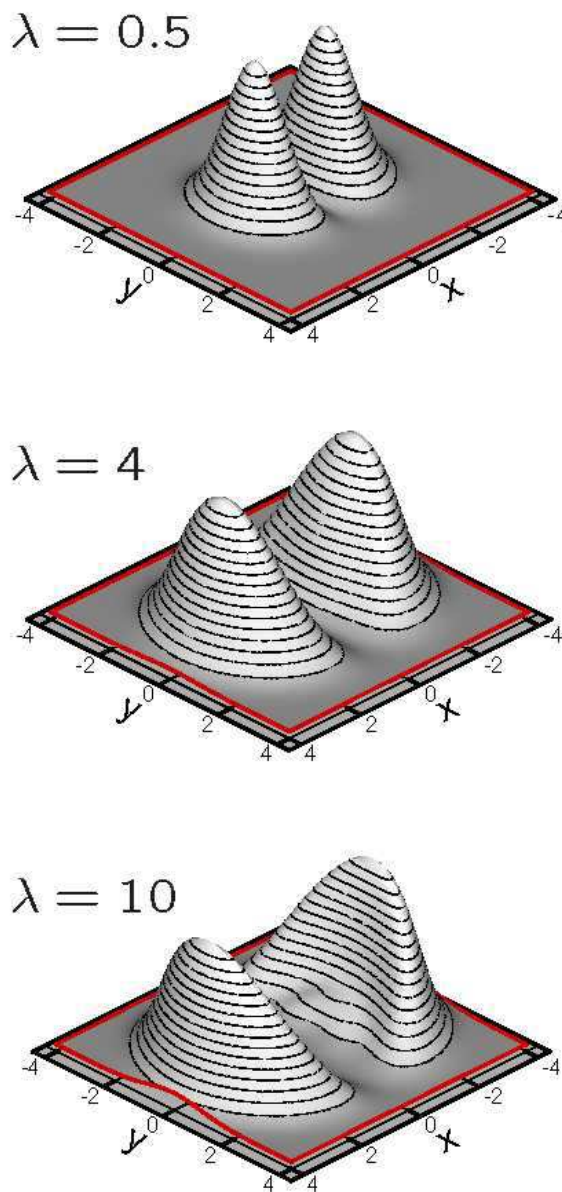


Fig. 2. Square modulus of the quasi-particle wave function in the quantum dot plane for three different values of the dimensionless parameter γ . This quantity is proportional to the STM signal when the electron number N fluctuates between 5 and 6. As γ increases (from top to bottom) the density decreases and the wave function shape evolves from a characteristic p-type Fock-Darwin orbital (top panel, $\gamma = 0.5$) into a complex figure peculiar of the "crystallized" phase (bottom panel, $\gamma = 10$). The wave function normalization is arbitrary and the length unit is the characteristic dot radius ℓ_D .

ticular, the specific filling sequence can be understood in terms of the consecutive filling of the s-orbital first, then one of the two p-orbitals of the second shell (Fig. 1), and eventually the other one. The above sequence differs from that expected according to Hund's rule, namely the third and fourth electrons should separately fill the two p-orbitals with parallel spins.¹²⁾ The deviation from the above rule is attributed to either piezoelectric effects or to a slight elongation of the InAs island shape.⁹⁾ However, many QDs were probed at once and the above interpretation cannot be regarded as definitive.

In a second experiment the imaging of InAs QD hole

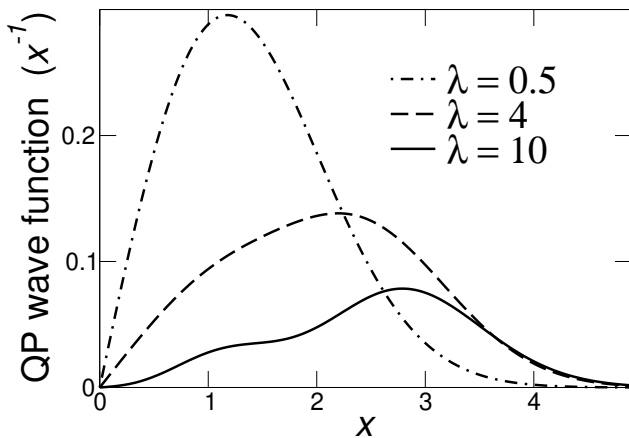


Fig. 3. Quasi-particle wave function vs. x ($y = 0$) for different λ -values. We use the same parameters as in Fig. 2 except that now the wave function normalization is absolute. As λ increases the total weight decreases from 0.97 ($\lambda = 0.5$) up to 0.15 ($\lambda = 10$).

wave functions was addressed.¹¹⁾ The authors observe an anomalous filling sequence up to 6 holes (s, s, p, p, d, d) and interpret it in terms of a generalized Hund's rule for the two p and the two d orbitals together, namely the total spin should be maximized as N increases as an effect of strong Coulomb correlation. Assuming reasonable hole parameters as $\lambda = 12.4$, $\sim I_0 = 25$ meV, $m = 0.3m_e$, we estimate, within the simple parabolic potential model, the key parameter λ to be 1.46. Such value is comparable to those of typical devices¹²⁾ showing "standard" Aufbau physics and it seems to us too small to support claims of qualitatively new correlation effects.¹⁷⁾ An alternative explanation of the filling sequence could be related to merely single particle effects arising from the complex hole band structure. Specifically, assuming orbital energies to be ordered as s, p, d and no shell degeneracy, then electrons should consecutively fill in such orbitals and Hund's rule would never hold. Such interpretation seems to be confirmed by independent theoretical work.²⁵⁾ Further measurements, as a function of the magnetic field parallel to z , could be useful to clarify the question.

From the above discussion it appears that experimental investigations of QP wave functions in regimes where correlation effects are significant are lacking so far. We hope that our results will stimulate further experiments.

6. Conclusions

In conclusion, we have shown that QP wave functions of QDs are extremely sensitive to electron-electron correlation, and may differ from single-particle states in physically relevant cases. This result is of interest to predict the real- and reciprocal-space wave function images obtained by tunneling spectroscopies, as well as the intensities of addition spectra of QDs. We believe that our findings will be important also for other strongly correlated systems, like e.g. nanostructures at surfaces.²⁶⁾

Acknowledgment

We thank A. Lorke and S. Heun for valuable discussions. This paper is supported by MIUR-FIRB RBAU01ZEM L, MIUR-COFIN 2003020984, I.T. INFN Calc.Par.2005, Italian Minister of Foreign Affairs, General Bureau for Cultural Promotion and Cooperation.

- 1) L. Jacak, P. Hawrylak and A. Wojs: Quantum dots, (Springer, Berlin, 1998).
- 2) D. Bimberg, M. Grundmann and N.N. Ledentsov: Quantum dot heterostructures, (Wiley, New York, 1999).
- 3) S.M. Reimann and M. Manninen: Rev. Mod. Phys. 74 (2002) 1283.
- 4) B. G. Randriah, Y.M. Niquet, B. Legrand, J.P. Nys, C. Priester, D. Stievenard, J.M. Gerard and V. Thierry-Mieg: Phys. Rev. Lett. 85 (2000) 1068.
- 5) O. Silob, D. Katz, Y. Cao and U. Banin: Phys. Rev. Lett. 86 (2001) 5751.
- 6) T. M. Altezopoulos, A. Bolz, C. Meyer, C. Heyn, W. Hansen, M. Morgenstern and R. Wiesendanger: Phys. Rev. Lett. 91 (2003) 196804.
- 7) E.E. Vdovin, A. Levin, A. Patane, L. Eaves, P.C. Main, Yu. N. Khanin, Yu. V. Dubrovskii, M. Henini, and G. Hill: Science 290 (2000) 122.
- 8) A. Patane, R. J. A. Hill, L. Eaves, P.C. Main, M. Henini, M. L. Zambano, A. Levin, N. Mori, C. Hamaguchi, Yu. V. Dubrovskii, E.E. Vdovin, D. G. Austing, S. Tanucha and G. Hill: Phys. Rev. B 65 (2002) 165308.
- 9) O. Silob, A. Lorke, D. Reuter and A. D. Wieck: Appl. Phys. Lett. 86 (2005) 092104.
- 10) M. Rontani and E. Molinari: Phys. Rev. B 71 (2005) 233106.
- 11) D. Reuter, P. Kailuweit, A. D. Wieck, U. Zeitler, O. Silob, C. Meyer, A. Lorke and J.C. Mann: Phys. Rev. Lett. 94 (2005) 026808, and private communication.
- 12) S. Tanucha, D. G. Austing, T. Honda, R. J. van der Hage and L. P. Kouwenhoven: Phys. Rev. Lett. 77 (1996) 3613.
- 13) R. C. Ashoori: Nature 379 (1996) 413.
- 14) J. Bardeen: Phys. Rev. Lett. 6 (1961) 57.
- 15) J. Tersoff and D. R. Hamann: Phys. Rev. B 31 (1985) 805; J. Tersoff: Phys. Rev. Lett. 57 (1986) 440.
- 16) The quantity is also known as the spectral density amplitude of the one-electron propagator resolved in real space. For analogous treatments in many-body tunneling theory see e.g. J. A. Appelbaum and W. F. Brinkman: Phys. Rev. 186 (1969) 464; T. E. Feuchtwang: Phys. Rev. B 10 (1974) 4121, and refs. therein.
- 17) M. Rontani, C. Cavazzoni, D. Bellucci and G. G. Oldoni: available at cond-mat (2005).
- 18) M. Rontani, S. Amaha, K. Muraki, F. Manghi, E. Molinari, S. Tanucha, and D. G. Austing: Phys. Rev. B 69 (2004) 85327.
- 19) M. Rontani, C. Cavazzoni and G. G. Oldoni: Comp. Phys. Commun. 169 (2005) 430.
- 20) Here we implemented a parallel version of our CI code, allowing for using a Fock-Darwin basis set as large as 36 orbitals, and for diagonalizing matrices of linear dimensions up to 10^6 . As a convergence test,¹⁷⁾ we could accurately reproduce QMC ground state energies up to $\lambda = 10$ and $N = 6$.²¹⁾
- 21) R. Egger, W. Hausler, C. H. Mak and H. G. Rabert: Phys. Rev. Lett. 82 (1999) 3320.
- 22) The dimensionless ratio is the QD analog to the density parameter r_s in extended systems.
- 23) F. Bolton and U. Rossler: Superlatt. Microstruct. 13 (1993) 139; V.M. Bedanov and F.M. Peeters: Phys. Rev. B 49 (1994) 2667.
- 24) M. Rontani, G. G. Oldoni, F. Manghi and E. Molinari: Europhys. Lett. 58 (2002) 555.
- 25) L. He, G. Bester and A. Zunger: cond-mat/0505330.
- 26) See e.g. P. Jarillo-Herrero, S. Sapmaz, C. Dekker, L. P. Kouwenhoven and H. S. J. van der Zant: Nature 429 (2004) 389.